NJC

Accepted Manuscript

This is an *Accepted Manuscript*, which has been through the Royal Society of Chemistry peer review process and has been accepted for publication.

Accepted Manuscripts are published online shortly after acceptance, before technical editing, formatting and proof reading. Using this free service, authors can make their results available to the community, in citable form, before we publish the edited article. We will replace this *Accepted Manuscript* with the edited and formatted *Advance Article* as soon as it is available.

You can find more information about *Accepted Manuscripts* in the Information for Authors.

Please note that technical editing may introduce minor changes to the text and/or graphics, which may alter content. The journal's standard Terms & Conditions and the Ethical guidelines still apply. In no event shall the Royal Society of Chemistry be held responsible for any errors or omissions in this *Accepted Manuscript* or any consequences arising from the use of any information it contains.

ROYAL SOCIETY OF CHEMISTRY

www.rsc.org/njc

ARTICLE TYPE www. rsc.org/xxxxxx | XXXXXXXX

On the properties of S···O and S···π noncovalent interactions: analysis on geometry, interaction energy and electron density

Fangfang Zhou, Ruirui Liu, Ping Li and Houyu Zhang*

Received Xth XXXXXXXXXX 20XX, Accepted Xth XXXXXXXXX 20XX
First published on the web Xth XXXXXXXXXX 200X
DOI: 10.1039/b000000x

Computational studies have been carried out to investigate the origin and magnitude of chemically and biologically important S···O and S···π interactions at the MP2/aug-cc-pVDZ level. All the model complexes involving S···O and S···π interactions exhibit the similar structures in which the O atom or π-system approaches the S atom from the backside of F-S bond (in the σ_S^* direction). The decomposition of interaction energy shows induction energy plays a dominant role in stabilizing the complexes, indicating that a primary source of such interaction is the charge transfer from the O lone pair or π-electrons to the S σ^* antibonding orbital. The topological analysis of electron density at the bond critical points (BCPs) reveals that S···O and S···π interactions in these complexes are pure closed-shell interactions in nature. Our results suggest that accurate quantum chemical calculations on models of noncovalent interactions may be helpful in understanding the structures of proteins and other complex systems.

Introduction

Noncovalent interactions involving sulfur (S) atoms are prevalent in chemical[1,2] and biological systems,[3–5] and play an important role in molecular recognition[6] and protein stabilization.[7–10] Among these interactions, a divalent sulfur, which acts as an electron acceptor, can adopt weak coordination to a proximate heteroatom oxygen (O)[11–17] and aromatic ring or unsaturated C–C bond (π).[18–21] Such nonbonded S···O and S···π interactions can control the molecular conformation, chemical and biological activity, as well as molecular assembly and packing structure in the solid state.[22–26] Thus a deep understanding on the nature of S···O and S···π interactions is undoubtedly of importance in both chemistry and life science.

Statistical database survey in terms of X-ray crystallographic and spectroscopic analyses has demonstrated the existence of nonbonded intra- and intermolecular S···O interactions in both organic sulfur compounds and proteins. The S–O distance observed in the crystal ranges from 2.77 to 3.16 Å, sometimes only marginally less than the sum of the van der Waals radii of sulfur and oxygen (3.25-3.30 Å).[27,28] Thus the similarity and discrepancy of structural features for S···O interactions in such long range remains to be illustrated. Moreover, the directionality of S···O interactions could be rather subtle, and the factors governing the directional preferences need to be figured out.[29,30] Although it is widely accepted that the orbital interaction of $n_O \rightarrow \sigma_S^*$ is of great importance for S···O interactions,[8,24,25] the nature of such interactions still need to be elucidated in more details at the microscopic level.

The complexes involving S···π interactions can be easily found in Brookhaven Protein Data Bank (PDB) and Cambridge Crystallographic Database (CCD).[18,31,32] Among these observations, the S atoms are more frequently found above the aromatic rings, which indicates that the noncovalent interactions between sulfur and the π-electron systems of aromatic rings could contribute to the protein stability.[10,19,20] Experimental inspections and theoretical studies have been carried out to investigate whether the genuine S···π interactions exist or not,[21] however, the origin of S···π interactions are still elusive. The electrons$(\pi) \rightarrow \sigma_S^*$ orbital interaction is proposed to be responsible for the S···π interactions. Since both π-electrons in the aromatic ring and empty *d*-orbital of sulfur are highly polarizable, the dispersion force is expected to be important for S···π interactions.[33] In addition, attractive electrostatic interaction could be also indispensable. The questions regarding how these forces affect the structures and to what extent contribute to the binding energy still need to be solved.

Both S···O and S···π interactions might involve the electron transfer from lone pair of oxygen and π-electrons of unsaturated C-C bond to the antibonding orbital of the sulfur atom. The electron density changes would be expected in the complexes in comparison to their non-interacting components. So to analyze the electron density, together with its topology and derived electrostatic properties, would provide valuable information in understanding S···O and S···π interactions. In experiment, high resolution X-ray diffraction experiment with

State key laboratory of supramolecular structure and materials, Jilin University, Changchun 130012, P.R. China. Fax: 86-431-85193421; Tel: 86-431-85168492; E-mail: houyuzhang@jlu.edu.cn

† Electronic Supplementary Information (ESI) available: [details of any supplementary information available should be included here]. See DOI: 10.1039/b000000x/

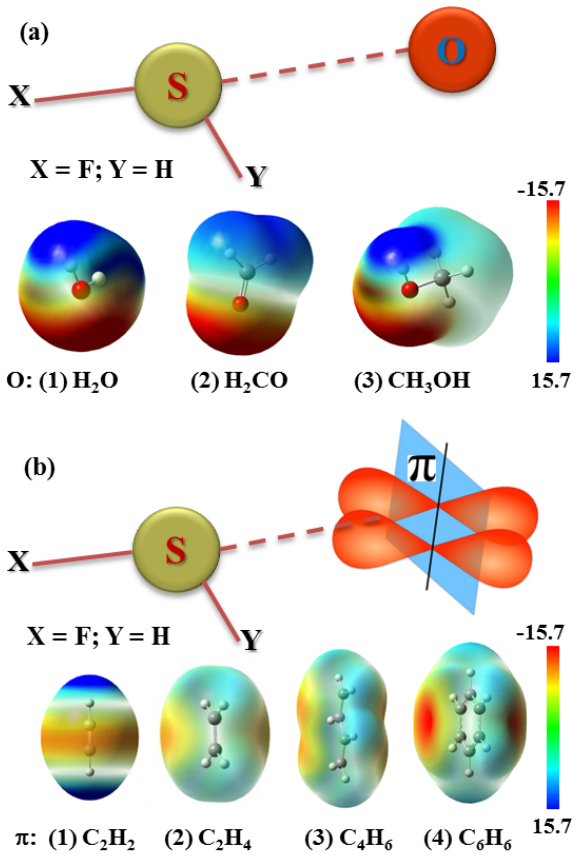

Fig. 1 Schematic illustrations of nonbonded (a) S···O and (b) S···π interactions investigated in this work. The oxygen-containing compounds and C–C π-electron systems are selected to pair with FHS, and their electrostatic surface potentials are also displayed (The red and blue color indicate negative and positive potentials, respectively, with the magnitudes of the electrostatic potentials from -15.7 to 15.7 kcal/mol.)

multipole refinements has been proven to be the most precise method at the electronic level.[34] From theoretical point of view, Bader's topological analysis of electron density is a widely used method to characterize intra- and intermolecular interactions.[35–37] The interaction energy which represents the associative strength between S and O (π) can be decomposed into distinct physically meaningful components. Such energy decomposition would help identify the dominant factor for stabilizing the complex and reveal the nature of S···O and S···π interactions.[38]

In this work, FHS is selected as a model electron acceptor molecule to interact with common and typical oxygen-containing compounds and C–C π-electron systems (shown in Fig. 1. We may assume without loss of generality that a divalent S atom is covalently bonded to two counteratoms (X and Y) with different electronegativity. Thus a nucleophilic O atom and π-electrons tend to selectively approach the S atom from the backside of either S–X or S–Y and the directional preference of S···O and S···π interactions can be distinguished and identified. For the oxygen-containing species, simple compounds namely water (H_2O), formaldehyde (H_2CO) and methanol (CH_3OH) are considered. In those compounds, sing bond of O–H, C–O and double bond C=O are commonly found in proteins. As for π-electron systems, acetylene (C_2H_2), ethene (C_2H_4), butadiene (C_4H_6) and benzene (C_6H_6) are taken into account because of distinct types of π-electrons. The selection of these oxygen-containing molecules and π-electron systems as electron donor was inspired by Scheiner's work[39] on the P···O and P···π noncovalent interactions. On the basis of a high level quantum chemical calculations on the model complexes, our main interest in the present work is to elucidate intrinsic structural features of S···O and S···π interactions, which would provide valuable information in protein structures and molecular design for drugs. To reach that end, we have carried out the comparative investigation on the geometries, electron density properties, electron transfer features as well as interaction energy decompositions for the model complexes. We aim to reveal the nature of S···O and S···π interactions in such complexes, and shed light on the basic knowledge of nonbonded weak S···O and S···π interactions on the implications in chemical and biological functions. Meanwhile, we make a direct comparison with the earlier work on P···O and P···π interactions. The extension of the previous work on P to S could represents a significant addition to our knowledge on such noncovalent intermolecular interactions.

Computational methods

All the calculations were performed with the Gaussian 09 package.[40] The geometries of model complexes were optimized at MP2[41]/aug-cc-pVDZ level, which is regarded as a reliable approach for evaluating weak intermolecular interactions.[42–53] Its accuracy can be comparable to that of CCSD with larger basis sets[54] and the energetic values are in good agreement with experimental data.[55] Harmonic vibrational frequencies were also calculated at the same level of theory on the optimized geometries to verify that the optimized model complexes were the minimum on the potential energy surfaces. The interaction energy was defined as the difference between the total energy of the complex and the sum of energies of two interacting monomers. Considering the basis set superposition error (BSSE) in MP2 theory, counterpoise (CP) technique developed by Boys and Bernardi[56] was employed to calculate the corrected binding energy. Natural bond orbital (NBO)[57,58] analysis was carried out via the procedures contained within Gaussian 09. The interaction energy was decomposed by the static and time-dependent DFT variant of symmetry-adapted perturbation theory (DFT-SAPT)[38,59–62] via the MOLPRO set of codes.[63] The gradient-regulated asymptotic correction approach[64] was used, where the exchange-correlation (XC) potential was calculated by the PBE0[65] functional. The identification of the orientation of the O lone pair, calculation of electron localization function (ELF)[66] and the electron density topological analysis were performed by Multiwfn program.[67]

Results and discussion

S···O interactions

The optimized model complexes involving S···O interactions are shown in Fig. 2. The geometrical parameters, interaction energies and NBO analysis results are collected in Table 1. All complexes exhibit structural similarity in which F–S bond stands far away from the O atom with the angle $\theta_{F-S\cdots O}$ within a narrow range between 166°and 170°. The O atom prefers to approach the S atom from the backside of F–S bond. The intermolecular distance $d_{S\cdots O}$ (in the range of 2.51 ∼ 2.63 Å) is shorter than the sum of their atomic van der Waals radii (3.32 Å), suggesting an existence of S···O interaction in each complex. The CP-corrected interaction energy ΔE^{CP} slightly increases by the change of the single bond in H_2O (5.26 kcal/mol) to the double bond in H_2CO (5.45 kcal/mol). While an apparent increment of interaction energy by 25% occurs upon replacing one of the H atoms of H_2O with a methyl group. Obviously, the increase of the interaction energy in these complexes is accompanied by the contraction in the distance of S···O contacts (as labelled in Fig. 2). In comparison to the previous study on P···O interaction[39], the S···O interaction energies increase by about 1 kcal/mol, indicating FSH is a stronger electron acceptor than FH_2P.

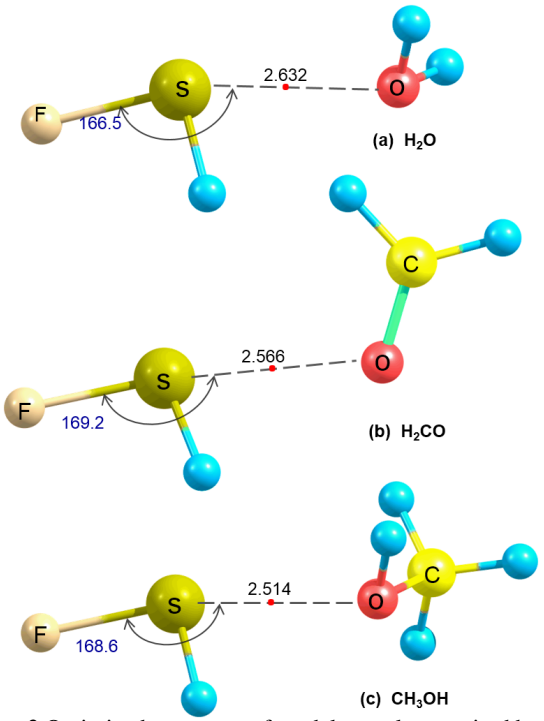

Fig. 2 Optimized structures of model complexes paired between FHS and oxygen-containing molecules. The S···O distances and the angles $\theta_{F-S\cdots O}$ are labelled for clarity. The red dots represent the bond critical points (BCPs) in S···O interactions. Distances in Åand angles in degs.

From the structural feature of model complex, it is noticeable that the divalent sulfur has a directional preference for interacting with an oxygen atom in both single and double bond. The angles $\theta_{F-S\cdots O}$ are quite close in all complexes, which is probably caused by the orientation of the lone pair of O atom and antibonding orbital of F–S bond. The orientations of the O lone pairs involved in S···O interactions are identified and the angles $\theta_{F-S\cdots n_O}$ are listed in Table 1. The values of $\theta_{F-S\cdots n_O}$ are very close to those of $\theta_{F-S\cdots O}$, indicating that the orientation of the O lone pair plays an important role in the determination of the structure for the complex. To further analyze the location of the lone pairs, the ELF of complexes are calculated and their ELF isosurface maps are displayed in Fig. 3. Two lone pairs appear in the vicinity of the O atom in each complex, as marked with dotted circles. One of the lone pairs exists in between S and O atoms, indicating that it must participate in the S···O interactions. The lone pair involved in S···O interaction is deformed, as it looks different from the other. Such deformation might be caused from two types of contacts: one is electrostatic repulsion between lone pairs of O and S atoms, resulting in that the O lone pair is located in the middle of two lone pairs of S and far away from them; another is charge transfer interaction from the O lone pair to the antibonding orbital of F–S bond. The electron density changes of the O lone pair would increase the induced dipole moment. Therefore, the electrostatic and induction forces would be expected in stabilizing the complexes. To this end, we turn to SAPT approach to decompose the interaction energy to account.

Table 1 Energetic (in kcal mol^{-1}), geometric (d in Å, θ in degs and Δd in mÅ) and electronic aspects (in me) for the complexes formed by FHS and oxygen-containing molecules

	H_2O	H_2CO	CH_3OH
ΔE^{CP}	-5.26(-4.03)[d]	-5.45(-4.78)	-6.58(-5.00)
$d_{S\cdots O}$	2.632	2.566	2.514
$\theta_{F-S\cdots O}$	166.5	169.2	168.6
$\theta_{F-S\cdots n_O}$ [a]	165.6	167.0	167.4
Δq[b]	18.1(11.6)	24.0(17.3)	28.7(19.0)
$E^{(2)}$[c]	10.63(7.69)	12.26(9.70)	15.29(10.91)
Δd_{F-S}	14.5	15.4	20.3

[a] Angle consisting of F-S bond and the O lone pair. [b] $n_O \rightarrow \sigma^*$(F-S) charge transfer, summed over both lone pairs of O atom. [c] NBO second-order perturbation energy corresponding to $n_O \rightarrow \sigma^*$(F-S). [d] Data in parentheses obtained from Ref 39, in which S is replaced by P with the same electron donors.

The stability of these complexes partly depends on the transfer of electron density from the O lone pair to the σ^* antibonding orbital of F–S bond.[68] NBO analysis can characterize such charge transfer process and give two important physical quantities: the amount of charge density transferred (Δq) from electron donor to acceptor and the concomitant second-order perturbation energy $E^{(2)}$. These two quantities are summarized in Table 1. The Δq increases in the order of $H_2O < H_2CO < CH_3O$, which is in accordance with the stabilization energy $E^{(2)}$. Both Δq and $E^{(2)}$ increase significantly compared with previous results on P···O interactions. An expected elongation in the intramolecular F–S bond is observed because of the extra charge density transferred into its σ^* antibonding orbital upon the formation of the complex. Stretches of F-S bond (Δd_{F-S}) are also given in

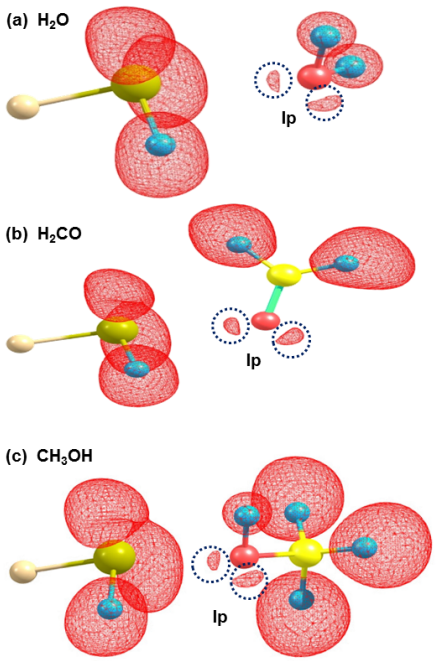

Fig. 3 Electron localization function (ELF) isodensity surface of 0.915 for the model complexes pairing FHS with oxygen-containing molecules.

Table 1, in which we can see that Δd_{F-S} correlates a bit more closely with $E^{(2)}$.

A decomposition of the total interaction energy into individual physically meaningful components, such as electrostatic (ES), induction (IND), dispersion (DISP) and their respective exchange counterparts, could help gain detailed information on the source of binding energy. The various constituent parts are given in Table 2, in

Table 2 SAPT decompositions of the interaction energy of the computed complexes (all in kcal mol^{-1})

	H_2O	H_2CO	CH_3OH
ES	-10.52(-8.38)[a]	-11.29(-11.16)	-15.40(-11.54)
EX	12.45	15.35	21.39
IND	-9.42(-4.87)	-12.70(-8.61)	-20.23(-9.16)
IND+EXIND	-1.68	-2.02	-2.69
DISP	-3.93(-3.25)	-5.11(-4.80)	-6.41(-5.43)
DISP+EXDISP	-3.15	-4.12	-4.92

[a] Data in parentheses obtained from Ref 39, in which S is replaced by P with the same electron donors.

which each term shows an increase in the order of $H_2O < H_2CO < CH_3O$. This remains in agreement with P$\cdots$O interactions in previous study[39](the corresponding data in parentheses). A large fraction of interaction energy is contributed from electrostatic and induction forces. In comparison to H_2O complex, the IND part becomes more important in stabilizing the CH_3OH complex. However, interacting with the same electron donors, the IND part play less important role for the acceptor FH_2P.[39] Relatively, DISP plays a minor role in these complexes, by about 60%-70% smaller than IND in magnitude. The contribution of electrostatic attraction can be understood from the electrostatic potential of O-containing compounds (displayed in Fig. 1). It can be seen that a negative (red) region where the O lone pair is located would approach to the backside of F–S bond. It is also verified in the ELF plots in Fig. 3 that the alignment of one of the O lone pairs with the F–S σ^* antibond could account for the more acute angle. Notably, the values of IND energy in Table 2 are rather similar to those of $E^{(2)}$ in Table 1, indicating that the charge transfer from the O lone pair to the F-S σ^* antibond should be largely responsible for the induction energy.

The topological analysis on the electron density could provide more information about the bonding nature in the intermolecular interaction. Electron density (ρ_b) and its Laplacian ($\nabla^2_{\rho_b}$) at bond critical points (BCPs) can identify and distinguish between a covalent and non-covalent bond. The value of ρ_b could represent the bond strength.[35] In addition, total electron energy density (H_b), which is the sum of kinetic energy density (G_b) and potential energy density (V_b) at BCPs would be another appropriate index for weak interactions on the energy basis.[35,69,70] Both $\nabla^2_{\rho_b}$ and H_b can be used to recognize a noncovalent pure closed-shell interaction. The well accepted feature for non-bonded interaction (*e.g.* hydrogen bond or charge-transfer interaction) is $\nabla^2_{\rho_{cp}} > 0$ and $H_b > 0$.[71] To investigate the S$\cdots$O interactions in the model complexes, analysis on the electron density on the BCPs of S$\cdots$O contacts has been carried out and some results are collected in Table 3. The BCPs in S$\cdots$O interaction (shown as a red dot in Fig. 2) indicate the existence of intermolecular interactions in these complexes. All the BCPs in S$\cdots$O interactions

Table 3 Topological and energetic properties at the S$\cdots$O bond critical points (BCPs) (all in a.u.)

	H_2O	H_2CO	CH_3OH
ρ_b	0.0196	0.0233	0.0264
$\nabla^2_{\rho_b}$	0.0769	0.0854	0.0944
G_b	0.0181	0.0208	0.0236
V_b	-0.0169	-0.0202	-0.0235
H_b	0.0012	0.0060	0.0001

are characterized by small ρ_b and positive $\nabla^2_{\rho_{cp}}$ and H_b. Thus we can classify these interactions as the pure closed shell interactions. The electron density at BCPs of S$\cdots$O interactions ranges from 0.0196 to 0.0264 a.u., suggesting an increasing interaction strength, which is in agreement with the interaction energy.

S$\cdots\pi$ interactions

The most stable structures of complexes of FHS with unsaturated π-electron systems are displayed in Fig. 4. Different from the complexes containing S$\cdots$O interactions, the π-electrons in C–C bond serve as electron donors in these complexes. The same structural feature as in S$\cdots$O interactions is found that F–S bond still appears away from the source of π-electrons. The most closest point in the π-electron systems interacting with S atom is neither any C atom nor the center of benzene, but the midpoint of one C–C bond (the X point

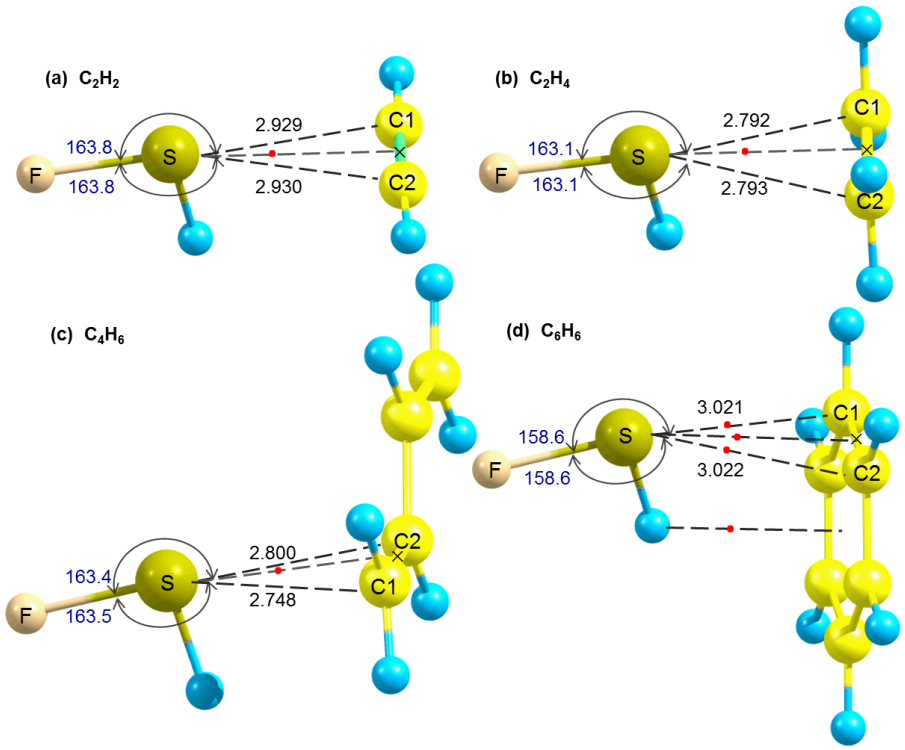

Fig. 4 Optimized structures of the model complexes pairing FHS with unsaturated π-electron systems. Distance in Åand angles in degs. In (a), (b) and (c), the red dots are the bond critical points. In (d), the red dots on the line connecting S and two C atoms are bond critical points; the red dots on the line connecting S and X and connecting H and the center of benzene are ring critical point and cage critical point, respectively.

marked in the bond center), which is rather similar to the structural features of P-containing electron acceptors.[39] The geometrical parameters, energies as well as NBO data are collected in Table 4 or labelled in Fig. 4. The distances between S atom and two interacting C atoms (marked as C1 and C2), together with the corresponding angles $\theta_{F-S\cdots C1(C2)}$, are almost identical in each complex with only exception for C_4H_6, probably because of the different chemical environments of these two C atoms in C_4H_6. The binding energies for these $S\cdots\pi$ interactions are in the range of 3.9 to 5.1 kcal/mol, which are a bit smaller than those in S$\cdots$O interactions. While they are larger by about 1 kcal/mol than those in P$\cdots\pi$ interactions.[39] The binding energy increases in the order of $C_2H_2 < C_2H_4 < C_4H_6 < C_6H_6$, mirrored by the gradual changes in a trend towards shorter distance of $d_{S\cdots X}$ with the exception of the fully aromatic benzene complex. The distance of $d_{S\cdots X}$ in benzene complex is 2.938 Å, apparently larger than those in the other three complexes. Another structural parameter is the angle $\theta_{F-S\cdots X}$, which is also singular in benzene complex. The $\theta_{F-S\cdots X}$ is 163.3^{o}for benzene complex, while these angels in the other three complexes are around 170^o, a bit larger than those in the S$\cdots$O interactions.

Both the exceptional distance $d_{S\cdots X}$ and angle $\theta_{F-S\cdots X}$ occur in benzene complex, which might be attributed to the existence of strong attractive S-H/π interaction. The electrons are abundant in the center of benzene ring, showing a negative electrostatic surface potential (as can be seen in Fig. 1); while the positive H atom of FHS is on the top of the benzene center. Therefore the attractive interaction between S-H and benzene could add to the binding energy of the complex. However, Such S-H/π interaction competes with the electron transfer interaction between π-electron system and the S atom. The competitive advantage of S-H/π interaction would make the FHS counterclockwise rotation in benzene complex, thus resulting in the exceptional $d_{S\cdots X}$ and $\theta_{F-S\cdots X}$. The structural feature in the benzene complex is very complicated, which is in agreement with previous findings.[39]

The NBO analysis results on the complexes are summarized in Table 4. Besides the charge transfer from C-C π-electrons to the F-S σ^* antibonding orbital (Δq_{FS} and $E^{(2)}_{FS}$), there also exists electron back-donation from the S lone pair to the C-C π^* antibond (Δq_{CC} and $E^{(2)}_{CC}$).[39] In both C_2H_4 and C_4H_6 complexes, Δq_{FS} and $E^{(2)}_{FS}$ give the roughly same values, so do for Δq_{CC} and $E^{(2)}_{CC}$ in the back donation process. These values are larger than those in C_2H_2 and C_6H_6. By comparison, all the data calculated here are 2$\sim$3 times larger than those corresponding values of P$\cdots\pi$ interactions with the only exceptional case of benzene.[39] Moreover, the stretches of the intramolecular F-S bond Δd_{F-S} are larger than those in C-C bond Δd_{C-C}, showing a consistency with the amounts of the charge transfer in two processes.

The plots of the ELF of complexes are shown in Fig. 5, in which

Table 4 Energetic (in kcal mol^{-1}), geometric (d in Å, θ in degs and Δd in mÅ) and electronic aspects (in me)of studied complexes formed by FHS and C-C π-containing molecules

	C_2H_2	C_2H_4	C_4H_6	C_6H_6
ΔE^{CP}	-3.95(-3.04)[c]	-4.50(-3.47)	-4.72(-4.11)	-5.07(-4.16)
$d_{S\cdots C1}$	2.930	2.792	2.800	3.022
$d_{S\cdots C2}$	2.929	2.793	2.749	3.021
$d_{S\cdots X}$	2.864	2.709	2.689	2.938
$\theta_{F-S\cdots C1}$	163.8	163.1	163.4	158.6
$\theta_{F-S\cdots C2}$	163.8	163.1	163.5	158.6
$\theta_{F-S\cdots X}$	169.3	170.6	171.5	163.3
$\Delta q_{FS}{}^a$	21.8(10.9)	44.0(18.9)	44.5(18.8)	21.5(31.3)
$E^{(2)a}_{FS}$	9.03(5.06)	17.06(8.01)	16.66(8.02)	6.25(7.68)
$\Delta q_{CC}{}^b$	9.2(3.8)	21.4(7.1)	21.4(7.6)	8.2
$E^{(2)b}_{CC}$	3.96(2.07)	8.10(3.52)	7.73(3.58)	2.33
Δd_{F-S}	13.7	24.5	27.0	13.0
Δd_{C-C}	2.9	8.1	8.8	2.7

[a] π(C-C)$\rightarrow\sigma^*$(F-S). [b] $n_S\rightarrow\pi^*$(CC) charge transfer. [c] Data in parentheses obtained from Ref 39, in which S is replaced by P with the same electron donors.

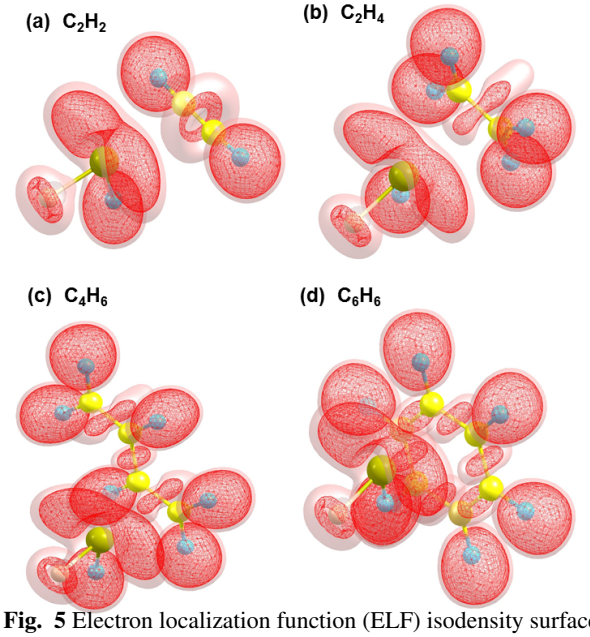

Fig. 5 Electron localization function (ELF) isodensity surface of 0.75 (outer) and 0.88 (inner) for the complexes involving FHS and π-electron systems.

the distinction of π-electron density in C-C bond can be clearly identified. To evading the direct repulsion with two lone pairs of S atom, the π-electron density in C-C bond is likely to appear in the middle of bond. Both electrostatic and charge-transfer interactions (the same as in S$\cdots$O interactions) deform the π-electron density in C-C bond, as can be seen clearly from ELF isosurface of 0.88. The loop-shaped π-electrons appear in C_2H_2 complex, while spindle-shaped π-electrons in the other three complexes. Both loop and spindle look not symmetrical, showing deformed electron density in the part against the S lone pairs.

The SAPT decomposed energy components are listed in Table 5. Induction force plays a dominant role in the stabilization of the complexes which is in agreement with the P$\cdots\pi$ interactions.[39] However, this is different from the halogen-π interactions where ES and DISP parts are more significant than the IND part.[72] Electrostatic and dispersion forces are minor and can be comparable in strength. The contribution of induction force increases doubly from the triply bonded C_2H_2 to the doubly bonded C_2H_4 and C_4H_6. In C_6H_6 complex, the energy components are comparable to those of C_2H_2 except the dispersion force, which is likely attributed to the high polarizability of the benzene and responsible for the strongest interaction energy of benzene complex.

The bonding nature in these complexes is also investigated through the topological analysis of the electron density at the BCPs in the S$\cdots\pi$ interactions (shown as a red dot in Fig. 4). The calculated data are collected in Table 6. The BCPs appear in between the S atom and midpoint of the C–C bond in the complexes except C_6H_6 case. The ρ_b value at the BCPs ranges from 0.0159 a.u. in C_2H_2 to 0.0240 a.u. in C_4H_6, indicating the gradual enhancement in binding strengthen. However, the smallest ρ_b (0.0129 a.u.) in S$\cdots$C contact in C_6H_6 complex is observed, which might be ascribed to the complexity of two types of weak interactions in the complexes. This can be verified from a ring critical point between the S atom and midpoint of the C–C bond, and cage critical point between H atom and center of benzene (shown in Fig. 4 (d)). The complicated weak interactions analyzed by topology of electron density can illustrate the possibility of completing of two interacting forces and interpret the special structural features in benzene complexes. The positive values of $\nabla^2_{\rho_b}$ and H_b reveal the nature of the pure closed-shell interactions in all complexes.

Comment on S$\cdots$O and S$\cdots\pi$ interactions

The complexes containing S$\cdots$O and S$\cdots\pi$ interactions are usually found in biological systems. The intramolecular nonbonded S$\cdots$O interaction in leinamycin can stabilize the sulfur heterocycle by altering the thiosulfinate ester conformation.[13] The theoretical study on the structural feature of leinamycin could help explain the X-ray data on leinamycin.[73] The fairly stable S$\cdots$O interactions are found in angiotensin II (AII) receptor antagonists.[74–76] Such interactions are responsible for both the conformation of these compounds and their activities.[12] Analysis on orbital interaction $n_O\rightarrow\sigma^*_S$ in these compounds may account for the structural features that S prefers to approach O on the orientation of the O lone pair. Our theoretical study on S$\cdots$O interactions could provide more detailed information to understand the structural feature and stability of biological systems. S$\cdots\pi$ interaction appears in the eye lens protein γ-crystallin[77] and can help protect the protein against radiation damage.[78] S$\cdots\pi$ interaction might play a significant role in stabilizing the fold conformations of the proteins.[79] Our calculated results show that S is more inclined to interact with π-electrons in proteins. S$\cdots\pi$ interactions are more complicated because many other interactions often coexist simultaneously and influence each other. Therefore, more cautions

Table 5 SAPT decompositions of the interaction energy of the complexes involving S$\cdots\pi$ interactions (all in kcal mol^{-1})

	C_2H_2	C_2H_4	C_4H_6	C_6H_6
ES	-8.96	-13.77	-13.70	-7.76
	(-6.94)[a]	(-9.62)	(-10.61)	(-6.75)
EX	14.15	24.61	26.45	14.45
IND	-13.35	-27.64	-29.04	-10.77
	(-7.77)	(-14.43)	(-16.65)	(-7.46)
IND+EXIND	-1.58	-3.05	-3.15	-1.37
DISP	-5.49	-8.33	-9.65	-8.11
	(-4.68)	(-6.54)	(-8.17)	(-7.60)
DISP+EXDISP	-4.36	-6.39	-7.47	-6.65

[a] Data in parentheses obtained from Ref 39, in which S is replaced by P with the same electron donors.

Table 6 Topological properties and energy properties at the S$\cdots\pi$ bond critical points (BCPs)(all in a.u.)

	C_2H_2	C_2H_4	C_4H_6	C_6H_6
ρ_b	0.0159	0.0225	0.0240	0.0129
$\nabla^2_{\rho_b}$	0.0536	0.0639	0.0646	0.0427
G_b	0.0112	0.0145	0.0150	0.0090
V_b	-0.0090	-0.0130	-0.0140	-0.0074
H_b	0.0022	0.0015	0.0010	0.0016

should be taken when dealing with these S$\cdots\pi$ interactions.

In comparison to previous work on P$\cdots$O and P$\cdots\pi$ interactions,[39] the S$\cdots$O and S$\cdots\pi$ interactions are stronger, showing that divalent S atom have a stronger electron-accepting ability than P atom. This is probably attributed to the more positive electrostatic potential (σ-hole) for divalent S along the extension of the F-S covalent bond. The calculated σ-hole potentials for S and P in FHS and FH_2P are 46 and 39 kcal/mol[30], respectively, which confirms our assumption. Induction energy in S$\cdots$O interactions makes more dominant contribution than that in P$\cdots$O interactions.

Conclusions

The investigation on FHS pairing with oxygen-containing compounds (H_2O, H_2CO, and CH_3OH) and π-electron systems (C_2H_2, C_2H_4, C_4H_6, and C_6H_6) provides a fully understanding on the nature of such interactions. Because the charge transfer interaction plays an important role (especially in the complexes involving π-electrons), induction force makes the dominate contribution to the interaction energy in these complexes. Notably, in the benzene complex, the case is more complicated due to the intervening of S-H/π interaction. However, in our present computational level, we are unable to separate these two interactions. The topological analysis at the BCPs reveals that the S$\cdots$O and S$\cdots\pi$ interactions in these complexes are the pure closed-shell interactions in nature.

Acknowledgement

We are grateful for the financial support from the National Nature Science Foundation of China (grant nos. 21073077 and 21173101).

References

1 S. Oae and J. T. Doi, *Organic Sulfur Chemistry: Structure and Mechanism*, CRC Press, Florida, 1991.
2 F. Bernardi and M. Angelo, *Organic Sulfur Chemistry: Theoretical and Experimental Advances*, Elsevier, Amsterdam, 1985.
3 R. Tanaka, Y. Oyama, S. Imajo, S. Matsuki and M. Ishiguro, *Bioorg. Med. Chem.*, 1997, **5**, 1389–1399.
4 S. Oae and T. Okuyama, *Organic Sulfur Chemistry: Biochemical Aspects*, CRC Press, Florida, 1992.
5 U. Adhikari and S. Scheiner, *ChemPhysChem*, 2012, **13**, 3535–3541.
6 G. R. Desiraju and V. Nalini, *J. Mater. Chem.*, 1991, **1**, 201–203.
7 L. M. Gregoret, S. D. Rader, R. J. Fletterick and F. E. Cohen, *Proteins*, 1991, **9**, 99–107.
8 M. Iwaoka, S. Takemoto and S. Tomoda, *J. Am. Chem. Soc.*, 2002, **124**, 10613–10620.
9 M. Iwaoka and N. Isozumi, *Molecules*, 2012, **17**, 7266–7283.
10 E. A. Meyer, R. K. Castellano and F. Diederich, *Angew. Chem. Int. Ed.*, 2003, **42**, 1210–1250.
11 E. Meyer, A. C. Joussef, H. Gallardo, A. J. Bortoluzzi and R. L. Longo, *Tetrahedron*, 2003, **59**, 10187–10193.
12 Y. Nagao, T. Hirata, S. Goto, S. Sano, A. Kakehi, K. Iizuka and M. Shiro, *J. Am. Chem. Soc.*, 1998, **120**, 3104–3110.
13 S. Wu and A. Greer, *J. Org. Chem.*, 2000, **65**, 4883–4887.
14 Y. Nagao, H. Iimori, S. Goto, T. Hirata, S. Sano, H. Chuman and M. Shiro, *Tetrahedron Lett.*, 2002, **43**, 1709–1712.
15 Y. Nagao, T. Honjo, H. Iimori, S. Goto, S. Sano, M. Shiro, K. Yamaguchi and Y. Sei, *Tetrahedron Lett.*, 2004, **45**, 8757–8761.
16 R. M. Minyaev and V. I. Minkin, *Can. J. Chem.*, 1998, **76**, 776–788.
17 F. T. Burling and B. M. Goldstein, *J. Am. Chem. Soc.*, 1992, **114**, 2313–2320.
18 R. J. Zauhar, C. L. Colbert, R. S. Morgan and W. J. Welsh, *Biopolymers*, 2000, **53**, 233–248.
19 K. S. C. Reid, P. F. Lindley and J. M. Thornton, *FEBS Lett.*, 1985, **190**, 209–213.
20 A. L. Ringer, A. Senenko and C. D. Sherrill, *Protein Sci.*, 2007, **16**, 2216–2223.
21 S. Yan, S. J. Lee, S. Kang, K.-H. Choi, S. K. Rhee and J. Y. Lee, *Bull. Korean Chem. Soc.*, 2007, **28**, 959–964.
22 S. Yamada and T. Misono, *Tetrahedron Lett.*, 2001, **42**, 5497–5500.
23 A. Esparza-Ruiz, A. Peña-Hueso, J. Hernández-Díaz, A. Flores-Parra and R. Contreras, *Cryst. Growth Des.*, 2007, **7**, 2031–2040.
24 R. E. Rosenfield Jr, R. Parthasarathy and J. D. Dunitz, *J. Am. Chem. Soc.*, 1977, **99**, 4860–4862.
25 T. N. G. Row and R. Parthasarathy, *J. Am. Chem. Soc.*, 1981, **103**, 477–479.
26 E. Ciuffarin and G. Guaraldi, *J. Org. Chem.*, 1970, **35**, 2006–2010.
27 A. Bondi, *J. Phys. Chem.*, 1964, **68**, 441–451.
28 A. F. Cozzolino, I. Vargas-Baca, S. Mansour and A. H. Mahmoudkhani, *J. Am. Chem. Soc.*, 2005, **127**, 3184–3190.
29 F. V. González, A. Jain, S. Rodríguez, J. A. Sáez, C. Vicent and G. Peris, *J. Org. Chem.*, 2010, **75**, 5888–5894.
30 P. Politzer, J. S. Murray and T. Clark, *Phys. Chem. Chem. Phys.*, 2013, **15**, 11178–11189.
31 F. C. Bernstein, T. F. Koetzle, G. J. B. Williams, E. F. Meyer Jr, M. D.

Brice, J. R. Rodgers, O. Kennard, T. Shimanouchi and M. Tasumi, *J. Mol. Biol.*, 1977, **112**, 535–542.
32 F. H. Allen, *Acta Cryst. B*, 2002, **58**, 380–388.
33 T. P. Tauer, M. E. Derrick and C. D. Sherrill, *J. Phys. Chem. A*, 2005, **109**, 191–196.
34 P. Coppens, *X-ray Charge Densities and Chemical Bonding*, Oxford University Press, USA, 1997.
35 R. F. W. Bader, *Atoms in Molecules: A Quantum Theory*, Oxford University Press, Oxford, U.K., 1994.
36 R. F. W. Bader, *Chem. Rev.*, 1991, **91**, 893–928.
37 U. Koch and P. L. A. Popelier, *J. Phys. Chem.*, 1995, **99**, 9747–9754.
38 R. Moszynski, P. E. S. Wormer, B. Jeziorski and A. van der Avoird, *J. Chem. Phys.*, 1995, **103**, 8058–8074.
39 S. Scheiner and U. Adhikari, *J. Phys. Chem. A*, 2011, **115**, 11101–11110.
40 M. J. Frisch, G. W. Trucks, H. B. Schlegel, G. E. Scuseria, M. A. Robb, J. R. Cheeseman, G. Scalmani, V. Barone, B. Mennucci, G. A. Petersson, H. Nakatsuji, M. Caricato, X. Li, H. P. Hratchian, A. F. Izmaylov, J. Bloino, G. Zheng, J. L. Sonnenberg, M. Hada, M. Ehara, K. Toyota, R. Fukuda, J. Hasegawa, M. Ishida, T. Nakajima, Y. Honda, O. Kitao, H. Nakai, T. Vreven, J. A. Montgomery, Jr., J. E. Peralta, F. Ogliaro, M. Bearpark, J. J. Heyd, E. Brothers, K. N. Kudin, V. N. Staroverov, R. Kobayashi, J. Normand, K. Raghavachari, A. Rendell, J. C. Burant, S. S. Iyengar, J. Tomasi, M. Cossi, N. Rega, N. J. Millam, M. Klene, J. E. Knox, J. B. Cross, V. Bakken, C. Adamo, J. Jaramillo, R. Gomperts, R. E. Stratmann, O. Yazyev, A. J. Austin, R. Cammi, C. Pomelli, J. W. Ochterski, R. L. Martin, K. Morokuma, V. G. Zakrzewski, G. A. Voth, P. Salvador, J. J. Dannenberg, S. Dapprich, A. D. Daniels, o. Farkas, J. B. Foresman, J. V. Ortiz, J. Cioslowski and D. J. Fox, *Gaussian 09 Revision D.01*, Gaussian Inc. Wallingford CT 2009.
41 C. Møller and M. S. Plesset, *Phys. Rev.*, 1934, **46**, 618–622.
42 E. Ruiz, D. R. Salahub and A. Vela, *J. Phys. Chem.*, 1996, **100**, 12265–12276.
43 R. M. Osuna, V. Hernández, J. T. L. Navarrete, E. D'Oria and J. J. Novoa, *Theor. Chem. Acc.*, 2011, **128**, 541–553.
44 J. M. Hermida-Ramón, E. M. Cabaleiro-Lago and J. Rodríguez-Otero, *J. Chem. Phys.*, 2005, **122**, 204315.
45 K. Riley, J. Murray, J. Fanfrlk, J. ez, R. Sol, M. Concha, F. Ramos and P. Politzer, *J Mol Model*, 2013, **19**, 4651–4659.
46 H. S. Biswal and S. Wategaonkar, *J. Phys. Chem. A*, 2009, **113**, 12774–12782.
47 K. E. Riley, B. T. Op't Holt and K. M. Merz Jr, *J. Chem. Theory Comput.*, 2007, **3**, 407–433.
48 M. G. Chudzinski, C. A. McClary and M. S. Taylor, *J. Am. Chem. Soc.*, 2011, **133**, 10559–10567.
49 I. Hyla-Kryspin, G. Haufe and S. Grimme, *Chem. Phys.*, 2008, **346**, 224–236.
50 S. Scheiner, *J. Phys. Chem. A*, 2011, **115**, 11202–11209.
51 U. Adhikari and S. Scheiner, *J. Phys. Chem. A*, 2012, **116**, 3487–3497.
52 S. Scheiner, *J. Chem. Phys.*, 2011, **134**, 164313.
53 P. R. Shirhatti, D. K. Maity, S. Bhattacharyya and S. Wategaonkar, *ChemPhysChem*, 2014, **15**, 109–117.
54 Q. Zhao, D. Feng, Y. Sun, J. Hao and Z. Cai, *Int. J. Quantum Chem.*, 2011, **111**, 3881–3887.
55 D. Hauchecorne, A. Moiana, B. J. van der Veken and W. A. Herrebout, *Phys. Chem. Chem. Phys.*, 2011, **13**, 10204–10213.
56 S. F. Boys and F. Bernardi, *Mol. Phys.*, 1970, **19**, 553–566.
57 A. E. Reed, F. Weinhold, L. A. Curtiss and D. J. Pochatko, *J. Chem. Phys.*, 1986, **84**, 5687–5705.
58 A. E. Reed, L. A. Curtiss and F. Weinhold, *Chem. Rev.*, 1988, **88**, 899–926.
59 H. L. Williams and C. F. Chabalowski, *J. Phys. Chem. A*, 2001, **105**, 646–659.
60 A. Heßelmann and G. Jansen, *Chem. Phys. Lett.*, 2002, **357**, 464–470.
61 A. Heßelmann and G. Jansen, *Chem. Phys. Lett.*, 2002, **362**, 319–325.
62 A. Heßelmann and G. Jansen, *Phys. Chem. Chem. Phys.*, 2003, **5**, 5010–5014.
63 H.-J. Werner, P. J. Knowles, G. Knizia, F. R. Manby and M. Schütz, *WIREs. Comput. Mol. Sci.*, 2012, **2**, 242–253.
64 M. Grüning, O. V. Gritsenko, S. J. A. Van Gisbergen and E. J. Baerends, *J. Chem. Phys.*, 2001, **114**, 652–660.
65 C. Adamo and V. Barone, *J. Chem. Phys.*, 1999, **110**, 6158–6169.
66 A. Savin, B. Silvi and F. Coionna, *Can. J. Chem.*, 1996, **74**, 1088–1096.
67 T. Lu and F. Chen, *J. Comput. Chem.*, 2012, **33**, 580–592.
68 S. Scheiner, *Phys. Chem. Chem. Phys.*, 2011, **13**, 13860–13872.
69 W. Nakanishi, T. Nakamoto, S. Hayashi, T. Sasamori and N. Tokitoh, *Chem. Eur. J.*, 2007, **13**, 255–268.
70 W. Nakanishi, S. Hayashi and K. Narahara, *J. Phys. Chem. A*, 2009, **13**, 10050–10057.
71 E. Espinosa, I. Alkorta, J. Elguero and E. Molins, *J. Chem. Phys.*, 2002, **117**, 5529–5542.
72 M. D. Esrafili, G. Mahdavinia, M. Javaheri and H. R. Sobhi, *Mol. Phys.*, 2014, **112**, 1160–1166.
73 N. Hirayama and E. S. Matsuzawa, *Chem. Lett.*, 1993, 1957–1958.
74 T. Hirata, J. Nomiyama, N. Sakae, K. Nishimura, M. Yokomoto, S. Inoue, K. Tamura, M. Okuhira, H. Amano and Y. Nagao, *Bioorg. Med. Chem. Lett.*, 1996, **6**, 1469–1474.
75 T. Hirata, S. Goto, K. Tamura, M. Okuhira and Y. Nagao, *Bioorg. Med. Chem. Lett.*, 1997, **7**, 385–388.
76 K. Tamura, M. Okuhira, H. Amano, K.-i. Inokuma, T. Hirata, I. Mikoshiba and K. Hashimoto, *J. CardioVasc. Pharmacol.*, 1997, **30**, 607–615.
77 T. Blundell, P. Lindley, L. Miller, D. Moss, C. Slingsby, I. Tickle, B. Turnell and G. Wistow, *Nature*, 1981, **289**, 771–777.
78 L. Summers, C. Slingsby, H. White, M. Narebor, D. Moss, L. Miller, D. Mahadevan, P. Lindley, H. Driessen and T. Blundell, *Ciba Found Symp.*, 1984, **106**, 219–236.
79 R. S. Morgan, C. E. Tatsch, R. H. Gushard, J. Mcadon and P. K. Warme, *Int. J. Pept. Protein Res.*, 1978, **11**, 209–217.

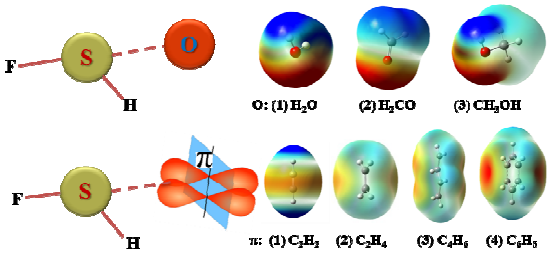

We report computational studies on the origin and magnitude of non-covalent S···O and S···π interactions.